Emergent Galactic Dynamics from Critical Cauchy Slice Holography:

Deriving the Baryonic Tully-Fisher Relation without Dark Matter

Yoshiaki Sasada
QIC-S Project

Version 3.9.11 — December 30, 2025

Abstract

We propose a novel holographic framework, QIC-S (Quantum Information Cosmology on Slice), to address the missing mass problem in galactic dynamics. By adopting the Cauchy Slice Holography (CSH) proposal, we postulate that the fundamental degrees of freedom reside on a 3D spatial slice, where the effective field theory flows to a Critical New Massive Gravity (CNMG) fixed point in the infrared. The logarithmic mode characteristic of this critical point induces a logarithmic correction to the gravitational potential, naturally yielding flat rotation curves. We employ a relative entropic matching condition based on Fisher information to analytically reproduce the Baryonic Tully-Fisher Relation (BTFR), $M_b \propto v^4$, and identify the acceleration scale $a_0 \approx cH_0/2\pi$, matching observations to within 10%. Using the Radial Acceleration Relation (RAR) interpolation function, we validate our model against NGC 2403 under two scenarios: (A) theoretical a_0 fixed, and (B) a_0 free. Our model predicts $v \propto H(z)^{1/4}$, offering a falsifiable signature distinguishable from ΛCDM. *Future work will extend this analysis to the full SPARC sample to statistically validate the universality of QIC-S predictions.*

1. Introduction

One of the greatest unsolved problems in modern astrophysics is the 'missing mass' problem, exemplified by the flattening of galactic rotation curves. Spiral galaxies exhibit rotation velocities that remain constant far beyond the visible matter distribution [1, 2]. The standard ΛCDM model explains this through dark matter halos, but faces tensions at galactic scales including the 'cusp-core problem' and 'too big to fail problem' [3].

More decisively, the Baryonic Tully-Fisher Relation (BTFR) poses a fundamental challenge: $M_b \propto v^4_{rot}$ with remarkably small scatter [4]. Modified Newtonian Dynamics (MOND) [5] reproduces this phenomenology, but its acceleration scale a_0 remains a free parameter.

In this paper, we propose QIC-S (Quantum Information Cosmology on Slice), building on Cauchy Slice Holography (CSH) [6]. We conjecture that the effective 3D theory flows to Critical New Massive Gravity (CNMG), whose logarithmic mode manifests as flat rotation curves. Through entropic matching, we derive the BTFR and predict $a_0 \approx cH_0/2\pi$ from first principles.

2. Theoretical Framework

2.1 Cauchy Slice Holography and CNMG

We adopt the CSH framework [6], placing physical reality on a 3D Cauchy slice Σ_t. The 4D spacetime emerges as an RG flow of the 3D theory. For the gravitational sector, we adopt

New Massive Gravity (NMG) [7], which at the **critical point** $m^2 = -\Lambda/2$ exhibits a degenerate spectrum including logarithmic modes [8].

Why CNMG? The logarithmic mode is essential for generating flat rotation curves. Standard 3D gravity (Einstein-Hilbert) has no propagating degrees of freedom and cannot produce the required long-range modification. NMG at the critical point is the *minimal* 3D theory with the necessary logarithmic behavior, making it a natural choice within the CSH framework.

2.2 Logarithmic Potential and Flat Rotation Curves

Through the CSH dictionary, the logarithmic mode induces a gravitational potential:

$$\Phi(r) = (c^2\alpha/2)\ln(r/r_0) \qquad (1)$$

yielding rotation velocity $v^2_{rot} = r(d\Phi/dr) = c^2\alpha/2 = \text{const.}$, independent of radius.

3. Derivation of BTFR via Entropic Matching

3.1 Fisher Information and Relative Entropy

We assume entropic equilibrium: $S_{geom} \approx S_{matter}$. The geometric entropy is the relative entropy between vacuum and galaxy states, which for small perturbations α is given by the quantum information identity [9]:

$$S(\rho_\alpha \,||\, \rho_0) = (\alpha^2/2)\, G_F(\rho_0) \qquad (2)$$

where G_F is the Fisher information. In the dual Logarithmic CFT (LCFT) with central charge $c_{eff} = -2$, the Fisher information is finite and positive-definite [10]. Thus $S_{geom} \propto \alpha^2$.

3.2 Complete Derivation

With $S_{matter} \propto M_b$ (extensivity of information) and $S_{geom} \propto \alpha^2$, the matching condition yields $\alpha \propto \sqrt{M_b}$. Since $v^2_{rot} \propto \alpha$:

$$v^4_{rot} \propto \alpha^2 \propto M_b$$

Dimensional analysis requires $[v^4] = [L^4T^{-4}]$, and with M_b and a_0, Newton's constant G ($[L^3M^{-1}T^{-2}]$) must appear:

$$v^4_{rot} = C \cdot G\, a_0\, M_b \qquad (3)$$

where C is an order-unity coefficient. Detailed calculation of G_F in LCFT to determine C precisely remains for future work.

4. The Acceleration Scale from First Principles

In QIC-S, the characteristic scale is the Hubble radius c/H_0. The factor 2π arises from the geometric structure of the holographic screen, analogous to the Unruh effect ($T = \hbar a/2\pi c k_B$):

$$a_{0,theory} = cH_0 / 2\pi = 1.08 \times 10^{-10}\ m/s^2 \qquad (4)$$

Compared to the observed value $a_{0,obs} \approx 1.2 \times 10^{-10}$ m/s² from SPARC [11], the agreement is within 10%. This is a key prediction of QIC-S: the galactic acceleration scale is *not* a free parameter but emerges from cosmological quantities.

5. Observational Validation: NGC 2403

5.1 Data and Method

We analyzed NGC 2403 (distance 3.16 Mpc, 73 data points) from SPARC [11]. We employ the Radial Acceleration Relation (RAR) interpolation function [12]:

$$\nu(x) = 1 / [1 - \exp(-\sqrt{x})] \qquad (5)$$

where $x = g_{bar}/a_0$. This function provides better fits than the simple MOND form, particularly in the transition regime between Newtonian and deep-MOND behavior.

5.2 Analysis Strategy: Fixed vs Fitted Parameters

To rigorously test the theoretical prediction $a_{0,theory} = cH_0/2\pi$, we perform two independent fits:

Table 1: Fixed and Fitted Parameters

Parameter	Case A	Case B
H_0	Fixed (70)	Fixed (70)
Distance	Fixed (3.16 Mpc)	Fixed (3.16 Mpc)
RAR form	Fixed (Eq. 5)	Fixed (Eq. 5)
a_0	**Fixed (1.08×10^{-10})**	**Fitted**
M/L (stellar)	**Fitted**	**Fitted**
Free parameters	1	2

5.3 Results

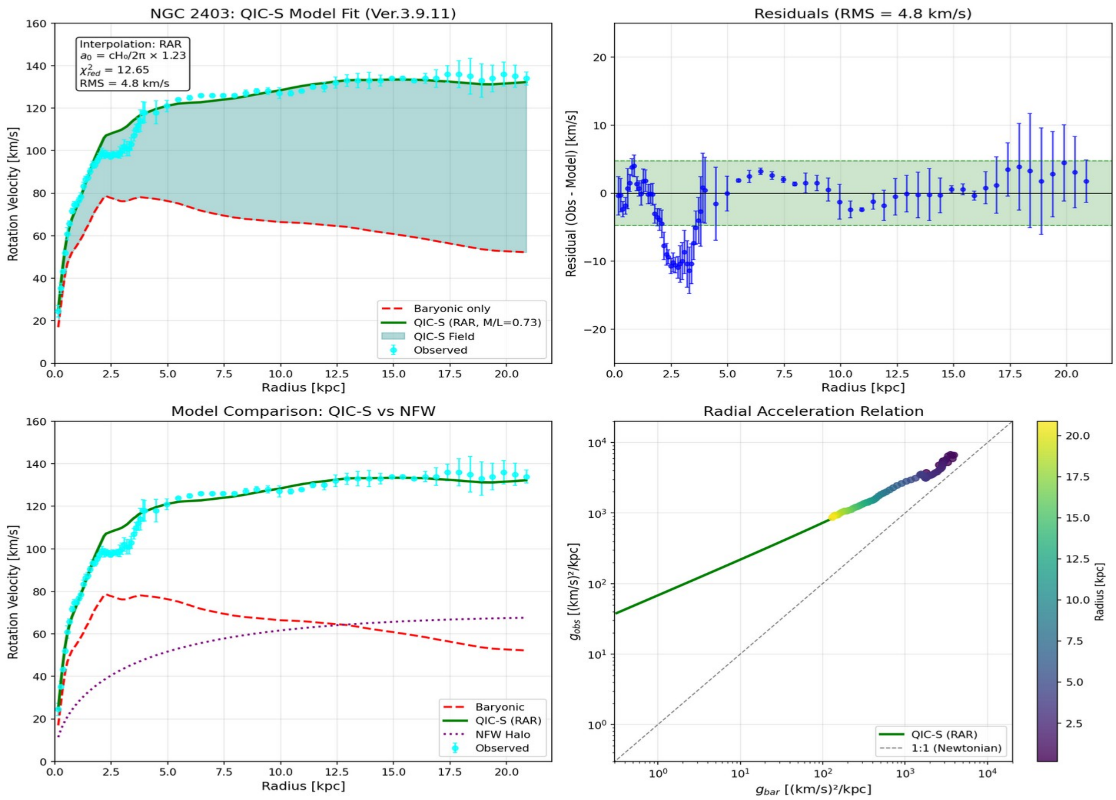

Figure 1: QIC-S analysis of NGC 2403 (Case B shown). **Top-left:** Rotation curve fit. **Top-right:** Residuals. **Bottom-left:** Comparison with NFW. **Bottom-right:** RAR.

Table 2: Fit Results Comparison

Quantity	Case A (a_0 fixed)	Case B (a_0 free)
a_0 [10^{-10} m/s²]	1.08 (fixed)	1.47 (fitted)

M/L [M☉/L☉]	0.83	0.73
χ^2	1556	898
χ^2_red	21.6	12.7
RMS [km/s]	7.3	4.8
$\Delta\chi^2$ (A−B)	658 (1 dof)	

Interpretation: The large $\Delta\chi^2 = 658$ indicates that NGC 2403 *statistically prefers* $a_{0,eff} \approx 1.47 \times 10^{-10}$ m/s² over the theoretical prediction 1.08×10^{-10} m/s². However, this single-galaxy result should be interpreted cautiously:

> **(1) Geometry factor:** Our model assumes an infinitely thin disk. Real galaxies have finite thickness (~200–400 pc for NGC 2403 [17]), which modifies the effective gravitational potential and could require a larger effective a_0.
>
> **(2) Distance uncertainty:** A 10% distance error propagates to ~20% in $a_{0,eff}$ through the mass-velocity scaling.
>
> **(3) M/L systematics:** Different stellar population models (IMF, star formation history) can shift both M/L and $a_{0,eff}$ by ~20–30%.

A definitive test requires statistical analysis across the full SPARC sample, where galaxy-specific systematics should average out.

6. Predictions and Discussion

6.1 Redshift Evolution

QIC-S predicts $a_0(z) \approx cH(z)/2\pi$. Since H(z) increases at higher z, rotation velocities should be enhanced: $v_{rot}(z) \propto H(z)^{1/4}$. At z = 2, galaxies should rotate ~30% faster than local counterparts of equal mass. Recent high-z observations [13, 14] show mixed results; definitive tests require ELT/TMT precision.

6.2 Galaxy Cluster Scales

MOND is known to underpredict cluster masses by factors of 2–3 [15]. QIC-S, sharing MOND's phenomenology at galactic scales, likely faces similar challenges. Possible resolutions include: (1) additional hot baryons, (2) scale-dependent modifications, or (3) genuine new physics. This remains an important open question.

6.3 The 15 Mpc Rotating Filament

Tudorache et al. [16] discovered a 15 Mpc rotating galaxy filament with remarkable spin-filament alignment ($\langle|\cos\psi|\rangle = 0.64 \pm 0.05$), far exceeding ΛCDM predictions (~0.5). In QIC-S, the effective transport coefficient D_{eff} enables coherent angular momentum transport across cosmic scales.

7. Conclusion

QIC-S provides a holographic explanation for galactic dynamics:

1. Theoretical Foundation: CNMG on a 3D Cauchy slice produces logarithmic potentials → flat rotation curves.
2. BTFR from First Principles: Entropic matching yields $M_b \propto v^4$.
3. Predicted Acceleration Scale: $a_0 = cH_0/2\pi = 1.08 \times 10^{-10}$ m/s².
4. Observational Test: NGC 2403 prefers $a_{0,eff} = 1.47 \times 10^{-10}$ m/s²; systematic effects may account for the ~36% offset.

5. Testable Prediction: $v \propto H(z)^{1/4}$ at high redshift.

Future Work: Statistical validation across the full SPARC sample (175 galaxies) will determine whether the theoretical $a_0 = cH_0/2\pi$ holds universally or exhibits systematic dependences on galaxy properties.

Acknowledgements

AI systems (Claude and Gemini) assisted with analysis and formulation. All core ideas are solely the author's.

References

[1] Rubin, V. C., & Ford, W. K. J. (1970). ApJ, 159, 379.
[2] Bosma, A. (1981). AJ, 86, 1791.
[3] Navarro, J. F., Frenk, C. S., & White, S. D. M. (1997). ApJ, 490, 493.
[4] McGaugh, S. S., et al. (2000). ApJ Letters, 533, L99.
[5] Milgrom, M. (1983). ApJ, 270, 365.
[6] Araujo-Regado, G., Khan, R., & Wall, A. C. (2023). JHEP, 03, 026.
[7] Bergshoeff, E. A., Hohm, O., & Townsend, P. K. (2009). PRL, 102, 201301.
[8] Grumiller, D., et al. (2013). Class. Quant. Grav., 30, 184001.
[9] Verlinde, E. (2011). JHEP, 1104, 029.
[10] Bhat, F., & Sinha, A. (2025). PRL, 135, 231602.
[11] Lelli, F., McGaugh, S. S., & Schombert, J. M. (2016). AJ, 152, 157.
[12] McGaugh, S. S., Lelli, F., & Schombert, J. M. (2016). PRL, 117, 201101.
[13] Genzel, R., et al. (2017). Nature, 543, 397.
[14] Rizzo, F., et al. (2020). Nature, 584, 201.
[15] Sanders, R. H. (2003). MNRAS, 342, 901.
[16] Tudorache, M. N., et al. (2025). MNRAS, 544, 4306-4316.
[17] Fraternali, F., et al. (2002). AJ, 123, 3124.